Transport, growth and stability of disturbances in weakly rarefied channel flows

Francesco Fedele, Darren L. Hitt*

Department of Mechanical Engineering, University of Vermont, Burlington, VT 05405, USA

Abstract

We examine the linear stability to axisymmetric disturbances in weakly rarefied flows ('slip regime') on the micro- and nano-scale. A semi-analytical solution of the Orr-Sommerfeld equation shows that pulsatile flow is linearly stable in the slip regime although a sudden change in the stability properties of the flow occurs at a critical value of the Knudsen number $Kn_{cr} = (2 - \sigma)/8\sigma$, where σ is the accommodation coefficient. Flow structures corresponding to the largest energy growth are toroidal vortex tubes that are transported diffusively and convectively by the mean flow. Transient energy growth is found to decrease at larger Knudsen numbers indicating that the Orr-Sommerfeld operator for slip flow is less non-normal compared to continuum-based no-slip flows.

Keywords: Slip flow; Stability; Pulsatile pipe flow; Orr-Sommerfeld operator; Galerkin projection; Non-normality; Vortex tubes; Energy growth

1. Introduction

The study of pulsatile tube flow, first considered in the context of arterial hemodynamics in the mid-1950s [1], has found renewed significance in its application to MEMS microfluidic engineering applications. A feature common to many of the devices described in the microfluidics literature that incorporate 'chip-level' pumping is that the flow is pulsatile in nature [2,3]. On the micro- and nano-scale the surface roughness of the channel walls can have greater impact on the flow behavior in contrast to their macro-scale counterparts; this is especially true for the case of rarefied (or 'slip') flows [4]. In addition to the potential generation of flow disturbances, the surface roughness also influences the velocity boundary condition for rarefied flows through tangential momentum accommodation coefficient σ [5].

Linear stability analyses of continuum-regime steady [6] and pulsatile flows [7,8] show that all of the eigenmodes are damped, although an initial energy growth of the flow perturbation can occur due to the non-normality of the Orr-Sommerfeld operator [9,10]. Transient growth is important if transition to turbulence is thought as emanating from 'by-pass transition' mechanisms [10]. In the following we extend the previous studies on pulsatile flow stability to the case of weakly rarefied flows ('slip regime') defined by Knudsen numbers ≤ 0.3.

2. Orr-Sommerfeld equation for a weakly rarefied pulsatile flow

We consider as an undisturbed state the fully-developed, pulsatile flow in a pipe of circular cross section of radius R driven by an imposed periodic pressure gradient $\partial P/\partial z$. The fully-developed streamwise velocity $W(r, t)$ satisfies the following initial boundary value problem

$$\rho \frac{\partial W}{\partial t} - \mu \frac{1}{r}\frac{\partial}{\partial r}\left(r\frac{\partial W}{\partial r}\right) = -\frac{\partial P}{\partial z}, \quad \frac{\partial P}{\partial z} = -[K_0 + K_\omega \exp(i\omega t)]$$

(1)

where μ is the dynamic viscosity, ρ is the density and ω is the frequency of the oscillating pressure gradient. For a weakly rarefied flow (or 'slip regime'), the velocity boundary condition is modeled as a first-order slip condition [11]

* Corresponding author. Tel.: +1 (802) 656 1940; Fax: +1 (802) 656 1929; E-mail: darren.hitt@uvm.edu

$$W|_{r=R} = \frac{2-\sigma}{\sigma}\lambda\frac{\partial W}{\partial r}\ |_{r=R} \tag{2}$$

where λ is the gas mean free path and σ is the tangential momentum coefficient (TMAC). The first-order slip condition (2) is valid provided the Knudsen number of the flow $Kn \equiv \lambda/2R \leq 0.3$ [11]. The value of σ is restricted to the range of [0, 1] whose lower and upper limits correspond to 'pure-slip' and 'no-slip,' respectively. The precise value of σ depends upon the fluid and the surface properties of the channel walls. Recent experiments by Arkilic et al. [5] using nitrogen, argon and carbon-dioxide and polished, single-crystal silicon walls have suggested a range of $\sigma = 0.75 - 0.85$.

The analytical solution of Eq. (1) subject to the boundary condition (2), when properly non-dimensionalized, is found as

$$W(r,t) = W_0 + W_1 \exp\ (it\ St) \tag{3}$$

$$W_0(r) = 1 - r^2 + 4\left(\frac{2-\sigma}{\sigma}\right) Kn \tag{4}$$

$$W_1(r,t) = \frac{4K_\omega}{i\ St\ Re\ K_0}$$

$$\left[1 - \frac{1}{1 - \left(2\frac{2-\sigma}{\sigma}Kn\right)\ i^{3/2}Wo\frac{J_1(i^{3/2}Wo)}{J_0(i^{3/2}Wo)}}\ \frac{J_0(i^{3/2}Wor)}{J_0(i^{3/2}Wo)}\right] \tag{5}$$

where the velocity scale is based on the steady Poiseuille flow component ($= K_0R^2/4\mu$), the length scale is the tube diameter, and the time scale is the oscillation period. The quantities Re and St are the Reynolds number and Strouhal numbers, respectively,

$$Re = \frac{\rho U\ R}{\mu} \qquad St = \frac{2R\omega}{U} \tag{6}$$

and are related to the Womersley number, $Wo = \sqrt{ReSt}$. The latter is generally interpreted as the ratio of oscillatory inertia to viscous forces.

We define a cylindrical coordinate system with z-axis along the streamwise direction and impose an axisymmetric velocity perturbation to the basic flow. Introducing a Stokes stream function of the form $\Psi(r, z, t) = \psi(r, t)e^{i\alpha z}$, with α the streamwise wave number, radial and streamwise velocity components of the perturbation are given by

$$u = -\frac{1}{r}\frac{\partial\Psi}{\partial z} = -\frac{\psi(r,t)}{r}i\alpha e^{i\alpha z}, \qquad w = \frac{1}{r}\frac{\partial\Psi}{\partial r} = \frac{1}{r}\frac{\partial\psi}{\partial r}e^{i\alpha z} \tag{7}$$

and the condition of incompressibility is automatically satisfied. Substitution of the basic flow (3)–(5) and the perturbation velocity (7) into the general Navier-Stokes equations yields, after neglecting nonlinear terms, the following Orr-Sommerfeld equation for the stream function ψ in dimensionless form [8]:

$$\mathcal{L}\psi_t - Wi\alpha^3\psi + i\alpha(-\psi\mathcal{L}W + W\mathcal{L}\psi) = Re^{-1}\mathcal{L}^2\psi \tag{8}$$

where $\mathcal{L}$ is defined by $\mathcal{L} = \partial^2/\partial r^2 - r^{-1}\partial/\partial r - \alpha^2$. The boundedness of the flow at the centerline and the slip condition at the wall of the pipe provide the boundary conditions:

$$\frac{1}{r}\psi, \quad \frac{1}{r}\frac{\partial\psi}{\partial r} < \infty \quad r \to 0^+ \tag{9}$$

$$\psi = 0, \qquad \frac{1}{r}\frac{\partial\psi}{\partial r} = 2\left(\frac{2-\sigma}{\sigma}\right) Kn\frac{d}{dr}\left(\frac{1}{r}\frac{\partial\psi}{\partial r}\right), \quad r = 1 \tag{10}$$

3. Galerkin projection method

We solve the Orr-Sommerfeld equation (8) by seeking an approximation stream function $\hat{\psi}(r, t)$ as

$$\hat{\psi}(r,t) = \sum_{k=1}^N a_k(t)\phi_k(r) \tag{11}$$

where $\{a_k(t)\}_{n=1}^N$ are time-dependent coefficients to be determined and the basis $\{\phi_n(r)\}_{n=1}^\infty$ is the set of eigenfunctions of the long-wave limit ($\alpha \to 0$) of the Orr-Sommerfeld equation (8). These basic functions satisfy the eigenvalue problem [8]

$$\tilde{\mathcal{L}}^2\phi_n = -Re\lambda_n\tilde{\mathcal{L}}\phi_n \tag{12}$$

subject to the boundary conditions (9)–(10). Here, $\tilde{\mathcal{L}} = r\partial/\partial r\ (r^{-1}\partial/\partial r)$ is a reduced operator and the eigenvalues are given by $\lambda_n = \chi_n^2/Re$, where χ_n are the roots of the eigenvalue relation

$$J_2(\chi) - 2sKn\chi J_1(\chi) = 0, \qquad s = \frac{2-\sigma}{\sigma} \tag{13}$$

and where $J_1(r)$ and $J_2(r)$ are the Bessel functions of first kind of order 1 and 2, respectively. One readily finds the solution for ϕ_n as

$$\phi_n(r) = \frac{\sqrt{2}r\left(r - \frac{J_1(\chi_n r)}{J_1(\chi_n)}\right)}{\chi_n\sqrt{1 - 2sKn\left(4 - 2\chi_n^2 sKn\right)}} \tag{14}$$

By means of a Galerkin projection, Eq. (8) yields the following system of periodic ordinary differential equations:

$$\mathbf{M}\frac{d\mathbf{a}}{dt} = [\mathbf{K} + \mathbf{H}\exp\ (it\ \mathrm{St})]\ \mathbf{a} \tag{15}$$

Here, $\mathbf{a}(t)$ is an ($N \times 1$) column vector whose n-th component is $a_n(t)$ and the entries of the ($N \times N$) constant matrices $\mathbf{M}$, $\mathbf{K}$, $\mathbf{H}$ are defined as follows:

$$(\mathbf{M})_{jk} = \delta_{jk} - \alpha^2 \langle \delta_j, \delta_k \rangle$$

$$(\mathbf{K})_{jk} = i\alpha^3 \langle W_0 \delta_j, \delta_k \rangle - i\alpha \langle W_0 \tilde{\mathcal{L}} \delta_j, \delta_k \rangle$$

$$(\mathbf{H})_{jk} = i\alpha^3 \langle W_1 \delta_j, \delta_k \rangle - i\alpha \left(\langle W_1 \tilde{\mathcal{L}} \delta_j, \delta_k \rangle - \langle \tilde{\mathcal{L}} W_1 \delta_j, \delta_k \rangle \right)$$

where δ_{jk} is the Kronecker delta and $\langle f, g \rangle = \int_0^1 fg \frac{dr}{r}$. The energy of the velocity field associated to the approximation stream function $\hat{\psi}$ is expressed as

$$\varepsilon(\hat{\psi}, t) = \frac{1}{2} \int_0^1 \left(\left| \frac{\partial \hat{\psi}}{\partial r} \right|^2 + \alpha^2 |\hat{\psi}|^2 \right) \frac{dr}{r} = \frac{1}{2} \mathbf{a}^*(t) \, \mathbf{M} \mathbf{a}(t) \tag{16}$$

where $\mathbf{a}^*$ denotes the Hermitian conjugate.

4. Stability and space-time evolution of an optimal perturbation

The time evolution of $\mathbf{a}(t)$, for any t, depends on the fundamental matrix $\mathbf{G}(t)$ that satisfies the system (15) with initial conditions $\mathbf{G}(0) = \mathbf{I}$, where $\mathbf{I}$ is the $N \times N$ identity matrix. The solution for $\mathbf{a}(t)$ can be written as

$$\mathbf{a}(t) = \mathbf{G}(t) \, \mathbf{a}(0) \tag{17}$$

where the vector $\mathbf{a}(0)$ defines the initial conditions. Following the arguments in [8] we compute the set of eigenvalues $\{\mu_k\}_{k=1}^N$ of the matrix $\mathbf{G}(T)$ where $T = 2\pi/$St is the dimensionless period of oscillations. The resulting solution is stable if all of the (complex)

characteristic exponents $\gamma_k = \ln \mu_k / T$ are such that Re$(\gamma_k) < 0$. Note that the matrix $\mathbf{G}(T)$ is non-normal. For the case of steady flow one has $\mathbf{G}(t) = \exp(-t \, \mathbf{M}^{-1} \mathbf{K})$ and γ_k is one the eigenvalues of $\mathbf{M}^{-1}\mathbf{K}$. The energy growth $\mathcal{G}(t)$ of the initial perturbation defined by the vector $\mathbf{a}(0)$ is given by (see Eq. (16))

$$\mathcal{G}(\mathbf{c}, t) = \frac{\varepsilon(\hat{\psi}, t)}{\varepsilon(\hat{\psi}, 0)} = \frac{\mathbf{a}(0)^* \mathbf{E}(t) \mathbf{a}(0)}{\mathbf{a}(0)^* \mathbf{E}(0) \mathbf{a}(0)}$$

where

$$\mathbf{E}(t) = \mathbf{G}(t)^* \mathbf{M} \, \mathbf{G}(t) \tag{18}$$

The optimal initial condition $\mathbf{a}_{opt}$ that gives the maximum growth $\mathcal{G}_{opt}(t)$ attained at time t satisfies the following eigenvalue problem:

$$\mathbf{E}(t)\mathbf{a}_{opt} = \mathcal{G}_{opt}(t)\mathbf{E}(0)\mathbf{a}_{opt} \tag{19}$$

Note that $\mathcal{G}_{opt}(t)$, as a function of t, can be regarded as the envelope of the energy evolution of individual optimal initial conditions $\mathbf{a}_{opt}$ giving the maximum growth $\mathcal{G}_{opt}(t)$ at time t (see also [10]).

4.1. Numerical results

We consider a perturbation with wavenumber $\alpha = 1$ and a strongly pulsatile forcing of the basic flow characterized by the ratio $K_\omega/K_0 = 2$. The characteristic exponents are plotted in Fig. 1 for a basic pulsatile flow state described by $Re = 1500$, $Wo = 38$ and $Kn = 0.1$.
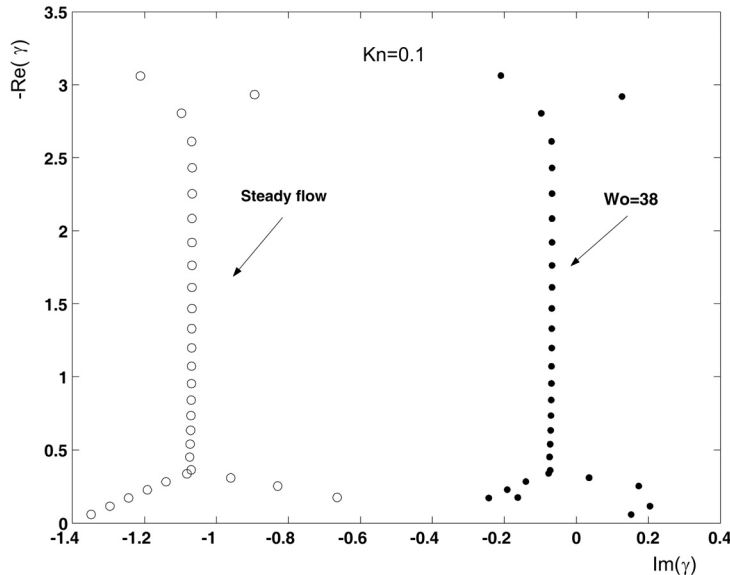

Fig. 1. Plots of the characteristic exponents $\{\gamma_k\}_{k=1}^N$ for $Kn = 0.1$, $Re = 1500$, $Wo = 38$, $K_w/K_0 = 2$ and wavenumber $\alpha = 1$. For comparison purposes, the plot of the eigenvalues of the steady Poiseuille flow ($Kn = 0.1$) is also shown. A Galerkin expansion consisting of $N = 30$ terms was used.
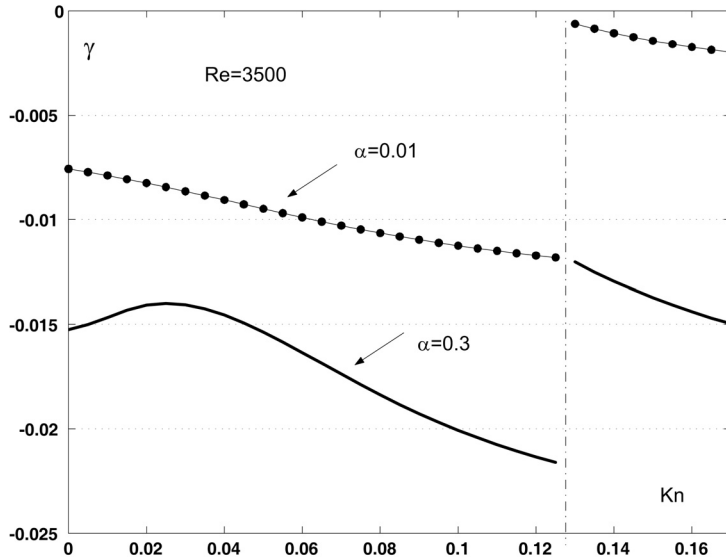
Fig. 2. Least stable eigenvalue for the case of steady Poiseuille flow as a function of the Knudsen number for different values of the streamwise wavenumber α and $\sigma = 1$.
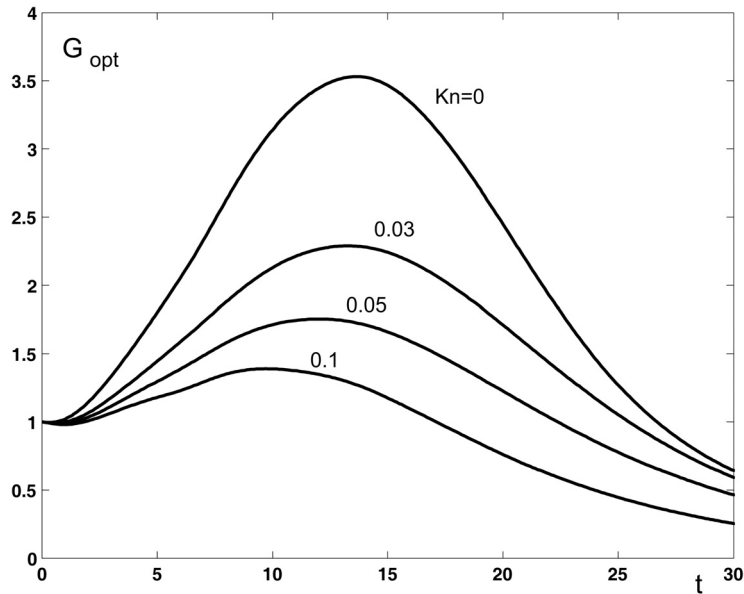

Fig. 3. Plots of $\mathcal{G}_{opt}(t)$ for different values of the Knudsen number for $Re = 3500$, $Wo = 30$, $\alpha = 1$ and $\sigma = 1$.

For comparison purposes, the plot of the eigenvalues of the steady flow is also shown ($Wo = 0$). As one can see, the negative characteristic exponents indicate the stability of the flow. The eigenmodes having the highest damping in Fig. 1 are spurious due to the numerical error in computing $\mathbf{G(T)}$ by the Runge-Kutta method.

Shown in Fig. 2 for the case of the steady Poiseuille flow ($Re = 3500$, $\sigma = 1$, $Wo = 0$), is the least stable eigenvalue as a function of the Knudsen number Kn for two different values of the streamwise wave number ($\alpha = 0.01$, 0.3). A jump discontinuity occurs at $Kn \simeq 1/8$, implying a non-smooth behavior of the spectral properties of the Orr-Sommerfeld operator. *Depending upon the values of both α and Kn the slip flow can be more*
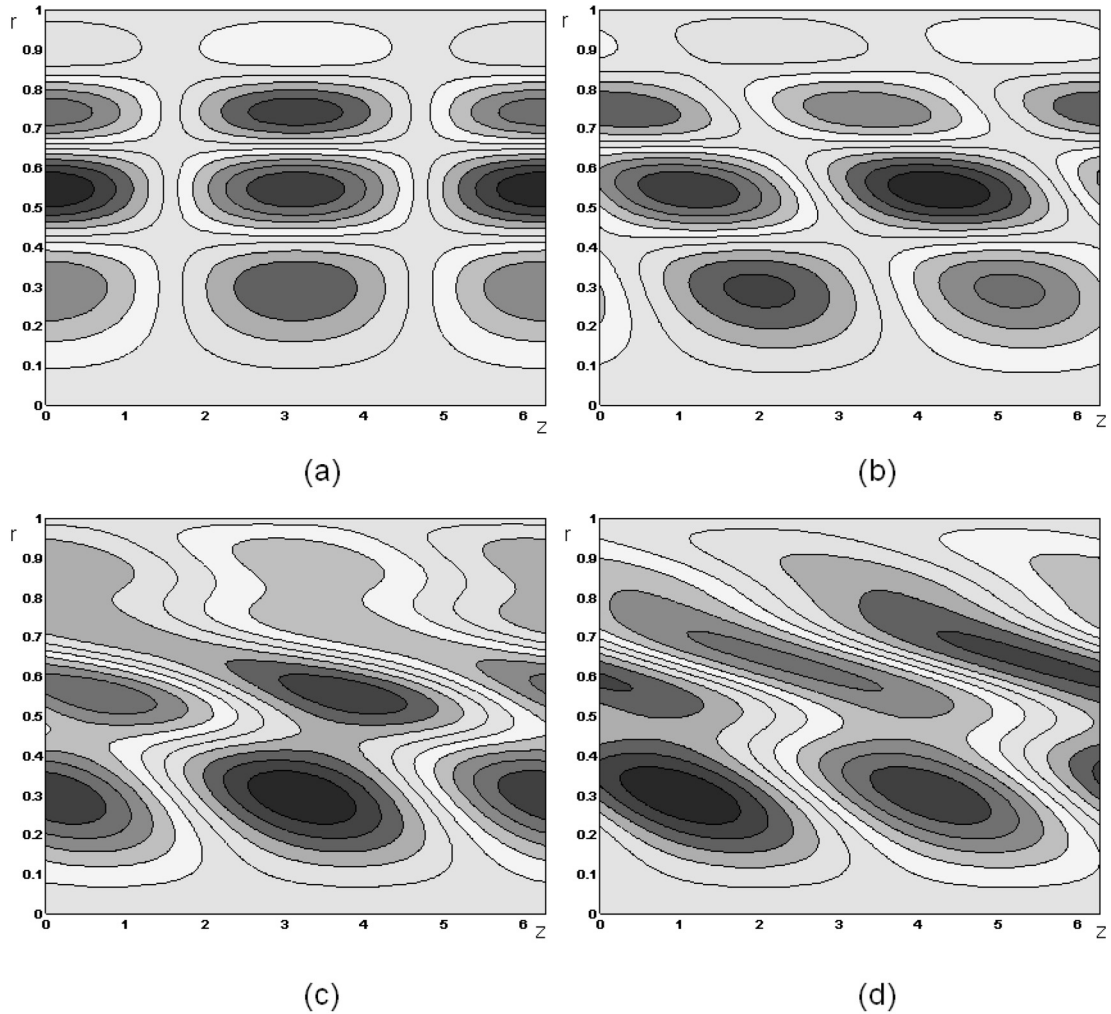
Fig. 4. The evolution of the stream function of the optimal disturbance for $Re = 3500$, $Kn = 0.1$ and steady flow conditions ($Wo = 0$). (a) $t = 0$ (b) $t = 3.9$, (c) 9.7, (d) 12.9.

or less stable than the no-slip flow counterpart (see Fig. 2). Note that this critical value of Kn is independent of wavenumber; moreover, it can be predicted analytically from the eigenvalue relation (13). The function $F(\chi) = J_2(\chi) - 2sKn\chi\, J_1(\chi)$ is even and admits the following Maclaurin series expansion for $\chi \ll 1$:

$$F(\chi) = \frac{1}{2}\left(\frac{1}{4} - 2sKn\right)\chi^2 + \frac{1}{4!}\left(-\frac{1}{4} + 3sKn\right)\chi^4 + O(\chi^6)$$

A non-trivial root

$$\chi_0 = \sqrt{12\frac{8sKn - 1}{12sKn - 1}}$$

exists such that $\chi_0 < 1$ only if $Kn > 1/8s$; for $Kn < 1/8s$ all non-trivial roots exceed unity. Thus, as Kn increases

starting from zero (continuum, no-slip), the least stable eigenvalue $\lambda_0 = \chi_0^2/Re$ is greater than Re^{-1} and varies continuously until a critical value $Kn_c = 1/8s$ is reached. For $Kn > 1/8s$, λ_0 suddenly becomes *less* than Re^{-1}. For the case of steady flow with $Re = 3500$ the plots of $\mathcal{G}_{opt}(t)$ versus t are reported for $Kn = 0, 0.03, 0.05$ and 0.1 in Fig. 3. One finds the largest energy growth $\mathcal{G}_{max}$ *decreases* as Kn increases and thus the Orr-Sommerfeld operator for slip flow is less non-normal than the case of no-slip flow ($Kn = 0$).

For the particular case of steady flow ($Kn = 0.1$ and $Re = 3500$) we computed the time evolution of the flow disturbance which gives the largest energy growth (see Fig. 4). The stream function of the initial flow perturbation is given in Fig. 4(a) whose flow structures are toroidal vortex tubes. In time the mean shear stress

tends to stretch the vortex tubes (Fig. 4(b)), so that at time $t = t_{max} = 9.7$ (Fig. 4(c)) the energy of the flow attains its largest growth ($\mathcal{G}_{max} \simeq 1.4$). Beyond this time the vortex tubes tend to migrate closer to the centerline where the effectiveness of the shear stress is diminished and a decay in time occurs due to viscous effects occurs (Fig. 4(d)).

5. Conclusions

In this paper we have examined the transport and energy growth of axisymmetric disturbances in weakly rarefied flows. The flow is found to be linearly stable under all conditions; however, depending upon the values of the perturbation wavenumber α and Kn the slip flow can be more or less stable than the no-slip flow counterpart. An abrupt change in the stability properties is found to occur at the critical value of the Knudsen number $Kn_{cr} = (2 - \sigma)/8\sigma$. For typical accommodation coefficients [5] this amounts to a Knudsen number of $Kn \simeq 0.17 - 0.33$, which lies within the assumed slip-regime of our model. The Orr-Sommerfeld operator for slip flow is less non-normal if compared to continuum-based no-slip flow because the transient energy growth decreases as the Knudsen number increases. The optimal flow disturbance giving the largest energy growth consists of toroidal vortex tubes that are stretched and convected by the mean flow until viscous effects become dominant and the structures diffusively decay.

Acknowledgments

References

[1] Hale JF, McDonald DA, Womersley JR. Velocity profiles of oscillating arterial flow with some calculations of viscous drag and the Reynolds number. J Physiol 1955;128:629–640.

[2] Geng X, Yuan H, Oguz HN, Prosperetti A. Bubble-based micropump for electrically conducting liquids. J Micromech Microeng 2001;11:270–276.

[3] Selverov KP, Stone HA. Peristaltically-driven channel flows with applications toward micromixing. Phys Fluids 2001;13:1837–1859.

[4] Liou WW, Fang Y. Modeling of the surface roughness effects for microchannel flows. In: Proc of 33rd AIAA Fluid Dynamics Conference, Orlando, FL, June 2003. AIAA paper 2003–3586.

[5] Arkilic EB, Breuer KS, Schmidt MA. Mass flow and tangential momentum accommodation in silicon micro-machined channels, J Fluid Mech 2001;437:29–443.

[6] Drazin PG, Reid WH. Hydrodynamic Stability. New York: Cambridge University Press, 1981.

[7] Tozzi JT, von Kerczek CH. The stability of oscillatory Hagen-Poiseuille flow. J Appl Mech 1986;53:187–192.

[8] Fedele F, Hitt DL, Prabhu RD. Revisiting the stability of pulsatile pipe flow. Eur J Mech B Fluids 2005;24:237–254.

[9] Reddy SC, Trefethen LN. Pseudospectra of the convection-diffusion operator. SIAM J Appl Math 1994;54(6):1634–1649.

[10] Schmid PJ, Hennigson DS. Stability and Transition in Shear Flows. New York: Springer, 2001.

[11] Karniadakis GEm, Beskok A. Micro Flows: Fundamentals and Simulations. New York: Springer, 2002.